Efficient phosphate recycling by adsorption on alkaline sludge biochar

Zehui Liu, Hongbo Liu, Yi Zhang, Eric Lichtfouse

Environmental Chemistry Letters
https://doi.org/10.1007/s10311-022-01527-5

Efficient phosphate recycling by adsorption on alkaline sludge biochar

Zehui Liu[1] · Hongbo Liu[1] · Yi Zhang[1] · Eric Lichtfouse[2]

Abstract

Large amounts of septic tank sludges from sanitation facilities are either landfilled or illegally dumped into the natural environment, leading to environmental pollution and waste of resources. This issue calls for advanced methods to recycle septic tank sludges such as sustainable adsorbents to recycle phosphorus, e.g., in agriculture, in the context of the circular economy. Here, we hypothesized that alkaline septic tank sludge biochar could be an efficient adsorbent to recycle phosphate from wastewater. We first prepared raw biochar by pyrolysis of septic tank sludge at 500 °C. Then, we prepared alkaline biochar by pyrolysis at 800 °C of mixtures of potassium hydroxide (KOH) and raw biochar at 3/1, 4/1 and 5/1 mass ratios. We studied biochar properties by scanning electron microscopy, X-ray diffraction and Fourier transform infrared spectroscopy, and we quantified adsorption of phosphates by biochars. Results show that phosphate adsorption highly increases with KOH content, from 27.83 mg/g for the raw biochar to 42.51 mg/g for the 5/1 KOH-biochar. This trend is explained by the increase in biochar surface area from 64.214 m^2/g for the raw biochar to 82.901 m^2/g for the 5/1 KOH-biochar, and by the improvement of the structural properties and surface morphology of KOH-biochars. Overall, alkaline biochar appears as a promising adsorbent to recycle phosphates from wastewaters.

Keywords Wastewater · Phosphate recovery · Septic tank sludge · Modified biochar · Potassium hydroxide

Abbreviations

KOH-free (raw) biochar	Biochar obtained by pyrolysis of septic tank sludge at 500 °C
3/1, 4/1, 5/1 KOH-biochars	Biochars prepared by pyrolysis of mixtures of potassium hydroxide and raw biochar at 3/1, 4/1, or 5/1 mass ratios
SEM	Scanning electron microscope
XRD	X-ray diffractometry
FTIR	Fourier transform infrared spectroscopy
BJH	Barrett–Joyner–Halenda
BET	Brunauer–Emmett–Teller method

Introduction

Approximately 2.7 billion people worldwide use pit latrines and septic tanks (Strande et al. 2014). The management of sludge from decentralized sewage treatment systems is a huge challenge, in particular in developing countries (Pandey and Jenssen, 2015). Actually, only a small amount of septic tank sludge is used in agriculture, and high load of untreated septic tank sludge is landfilled with domestic waste or illegally dumped into rivers or open spaces, due to the lack of systematic treatment facilities, which seriously threatens the environment and public health (Krueger et al. 2020).

Recycling of septic tank sludge is under active research. Methods such as gasification, hydrothermal carbonization and combustion are in development for the recycling of septic tank sludge (Recalde et al. 2018; Strande et al. 2017). For instance, biochar can be prepared using septic tank sludge as raw material (Bond et al. 2018). This biochar can be used

Zehui Liu and Hongbo Liu contribute equally to this work.

✉ Hongbo Liu
Liuhb@usst.edu.cn

Eric Lichtfouse
eric.lichtfouse@gmail.com

[1] School of Environment and Architecture, University of Shanghai for Science and Technology, 516 Jungong Road, Shanghai 200093, China

[2] Aix-Marseille University, CNRS, IRD, INRA, CEREGE, 13100 Aix en Provence, France

both as an adsorbent to recycle wastewater phosphorus and as a soil amendment to improve soil properties and sequester carbon. Indeed, phosphorus is a major element for plant growth in aquatic systems (Bizsel and Uslu, 2000).

Excessive accumulation of phosphorus in natural waters causes serious environmental problems such as the proliferation of phytoplankton, causing a decrease in oxygen content of water bodies and, in turn, the deterioration of water quality and aquatic life. Due to the inefficient natural recovery of phosphorus, the temporary generation of precipitation in the sediment and then its release into the water body again leads to the enrichment of phosphorus in the water body and highly promotes eutrophication (Li et al. 2013). Eutrophication is a global environmental problem. Indeed, with rapid urbanization, industrialization and intensification of agricultural production, the rate of nutrient input into water bodies has increased, highly accelerating eutrophication in water bodies (Cheng and Li, 2006). Furthermore, phosphorus is a non-renewable resource, and the over-exploitation of phosphorus resources by humans has led to a decrease in phosphorus resource stocks (Nguyen et al. 2016; Sheperd et al. 2016, Ye et al. 2016, Omwene and Kobya. 2018; Xu et al. 2019, Lei et al. 2020). Therefore, in the context of the circular economy, phosphorus recovery from wastewater could reduce environmental pollution and provide new options for the sustainable use of phosphorus resources (Huang et al. 2017; Wang et al. 2020a).

The removal and recovery of phosphorus from wastewaters require methods of low cost, high efficiency and convenient operation (Ahmad et al. 2014; Fang et al. 2015b; Guo et al. 2018). For instance, biochar produced by thermal decomposition of biomass is a promising adsorbent due to its abundant surface area with functional groups that can combine with aqueous chemicals (Sika and Hardie. 2014; Cha et al. 2016; Isa et al. 2022; Wang et al. 2022). Biochar from *Typha latifolia*, pine wood, peanut shells and corn stover have been used to remove phosphate from water, yet little is known on the use of biochar from septic tank sludge for phosphorus adsorption (Qiu and Duan. 2019; Wu et al. 2019; Feng et al. 2017).

Biochar from septic tank sludge should be an efficient adsorbent to recover phosphorus from wastewater because this biochar contains magnesium and iron (Fang et al. 2015a). Moreover, alkaline treatment of biochar with potassium hydroxide (KOH) facilitates the formation of pores, chemical functionalization, and increases the specific surface area, thus improving the efficiency of biochar for phosphorus adsorption in wastewater (Wang et al. 2020b; Bashir et al. 2018; Liu et al. 2018). At an activation temperature of 400–600 °C, potassium hydroxide and carbon produce potassium carbonate at high temperatures. When the temperature rises at more than 700 °C, KOH is gradually generated through three pathways: decomposition of potassium carbonate, reaction of potassium carbonate with carbon, and reaction of potassium with carbon dioxide (Lozano-Castelló et al. 2007). The gas generated during the activation process escapes from the carbon matrix and forms pores. The most important effect of the alkaline treatment with potassium hydroxide is the destruction of the carbon layer structure in the biomass. On the one hand, potassium hydroxide is able to react with functional groups at the edges of the aromatic lamellae, thus facilitating the formation of new aromatic hydrocarbons in the vertical direction of the carbon layer. On the other hand, potassium vapor diffuses between the aromatic lamellae, causing distortion and deformation of the carbon layer and creating new pores. The use of potassium hydroxide would also be beneficial to agriculture because potassium is a major plant nutrients and some acidic soils require alkaline treatment for better plant growth or pest inactivation. Therefore, here we studied the adsorption of phosphate with KOH-modified sludge biochar prepared by pyrolysis (Scheme S1).

Experimental

Instruments and reagents

Chemicals used such as potassium dihydrogen phosphate, sulfuric acid, sodium hydroxide, sodium molybdate, ascorbic acid and potassium persulfate were with chemical pure grade. Analyses were conducted using the following instruments: THZ-98AB thermostatic oscillator, DHG-9145A blast drying oven and DZF-6021 vacuum drying oven (Shanghai Yiheng Scientific Instrument Co., LTD.); FE20 pH meter and PL203 electronic balance from Mettler Toledo Instruments Shanghai Co., LTD.; SLG1100-60 tube furnace (Shanghai Shengli Test Instrument Co., LTD.); UV–visible spectrophotometer UV-2600 (Shimadzu, Japan); pore size analyzer 3H-2000 PS4 (Bestech China Instrument Co., LTD.).

Preparation of the modified biochar materials

Septic tank sludge to prepare biochar materials was obtained from the septic tank of a public toilet in Yangpu District, Shanghai China. The septic tank sludge is firstly cleaned with 1 mol/L hydrochloric acid for 1.5 h and then rinsed until neutrality and dried. Subsequently, 50 g of septic tank sludge was weighed in a quartz boat and inserted into a tubular furnace for 1 h pyrolysis under nitrogen atmosphere at 500 °C. The obtained pyrolytic biochar sample is abbreviated as KOH-free biochar.

Modified biochar samples were prepared by grinding biochar to potassium hydroxide solid in a certain proportion (KOH/ biochar mass ratios of 3/1, 4/1 and 5/1 respectively),

impregnated with pure water for 24 h and then dried in an oven at 85 °C. The KOH-biochar mixture is then pyrolyzed for 1.5 h in a tube furnace under nitrogen atmosphere at 800 °C. After cooling to room temperature, the solid is finally neutralized by adding 1 M hydrochloric acid and then dried. The obtained modified biochar is abbreviated as 3/1 KOH-biochar, 4/1 KOH-biochar and 5/1 KOH-biochar respectively, according to the mass ratios of potassium hydroxide and biochar.

Characterization of biochar materials

Scanning electron microscope (SEM) was used to observe the microstructure of the sample surface, including pore structure and surface morphology, with magnification from 50,000 to 200,000 times. Phase analysis of X-ray diffraction (XRD) was used to assess the crystalline structure, with diffraction angle ranging from 2° to 90°, the test speed of 6°/min and scan step size of 0.02°. Scans are finally analyzed using the MDI Jade v6.5 software. Surface groups were qualitatively analyzed by the Fourier transform infrared spectroscopy (FTIR) from 500 to 4000 cm^{-1}. For FTIR analysis, the sample is mashed into powder, mixed with KBr, tableted and then analyzed. Di-nitrogen (N_2) adsorption and desorption isotherms were measured by a specific surface area and pore size analyzer 3H-2000 PS4 Bayside, China. Mesopore volume and total pore volume were calculated using the Barrett–Joyner–Halenda (BJH) method for nitrogen adsorption at p/p_0 of 0.98, while specific surface area was calculated using the Brunauer–Emmett–Teller method (BET).

Isothermal and kinetic adsorption experiments

Isothermal investigations: Approximately 0.1 g each of biochar samples was weighed and put into several 250-ml conical flasks, and afterward, 50 mL of potassium phosphate monobasic (KH_2PO_4) solutions with concentrations of 10, 25, 30, 40, 50, 75, 100, 150, and 200 mg/L was added. The flask was placed in a constant-temperature oscillating incubator with a rotating speed of 180 rpm for 24 h at 30 °C. After oscillation, the supernatant was filtered through a 0.45 μm microporous membrane. The concentration of phosphorus in the solution was determined by the ultraviolet spectrophotometry at a 700 nm wavelength. The different concentrations of KH_2PO_4 solution were made in triplicate.

Kinetic investigations: Approximately 0.1 g each of biochar samples was weighed and put into 250-ml conical flasks and 50 mL of KH_2PO_4 solution with a concentration of 50 mg/L added in turn. The concentration of phosphorus in the solution was determined according to the same procedure. The supernatant samples of different time points of 10, 30, 60, 120, 180, 240, 480, 600, 720, and 1440 min were filtered through a 0.45 μm microporous membrane respectively. Three replicates were taken for different sampling times.

Isothermal and kinetic adsorption models

The Langmuir and Freundlich isothermal adsorption equations were used to fit the experimental data (Wu et al. 2020). Adsorption equations used are as follows:

Langmuir isothermal adsorption equation:

$$q_e = \frac{QK_LC_e}{1 + K_LC_e} \tag{1}$$

Freundlich isothermal adsorption equation:

$$qe = K_F C_e^{\frac{1}{n}} \tag{2}$$

where qe is the unit mass of adsorbent to achieve adsorption; Q is the maximum adsorption capacity, mg/g; C_e is the concentration of phosphorus at equilibrium, mg/L; K_L, K_F, and n are all constants.

The quasi-first-order kinetic equation and quasi-second-order kinetic equation were used to fit the experimental data (Wu et al. 2020).

Quasi-first-order kinetic equations:

$$q_t = q_e(1 - e^{-k_1 t}) \tag{3}$$

Quasi-second-order kinetic equations:

$$\frac{t}{q_t} = \frac{1}{k_2 q_e^2} + \frac{1}{q_e}t \tag{4}$$

where q_t is the adsorption capacity at time t, mg/g; q_e refers to the adsorption capacity of adsorbent per unit mass when reaching adsorption equilibrium, mg/g; t is the adsorption time, min; K_1 and K_2 are the constants.

Results and discussion

We studied the adsorption of phosphates by KOH-modified septic tank sludge biochar. The following sections present biochar characterization, phosphate recovery by adsorption, and a comparison of phosphate adsorption performance with the literature.

Characterization of the prepared biochar materials

The microscopic morphology of biochar is shown in Fig. 1. The surface of KOH-free biochar is rough and granular, and the pore structure is concentrated on the surface. This may be due to the decomposition of mineral components in the sludge into particles attached to the surface of biochar. The

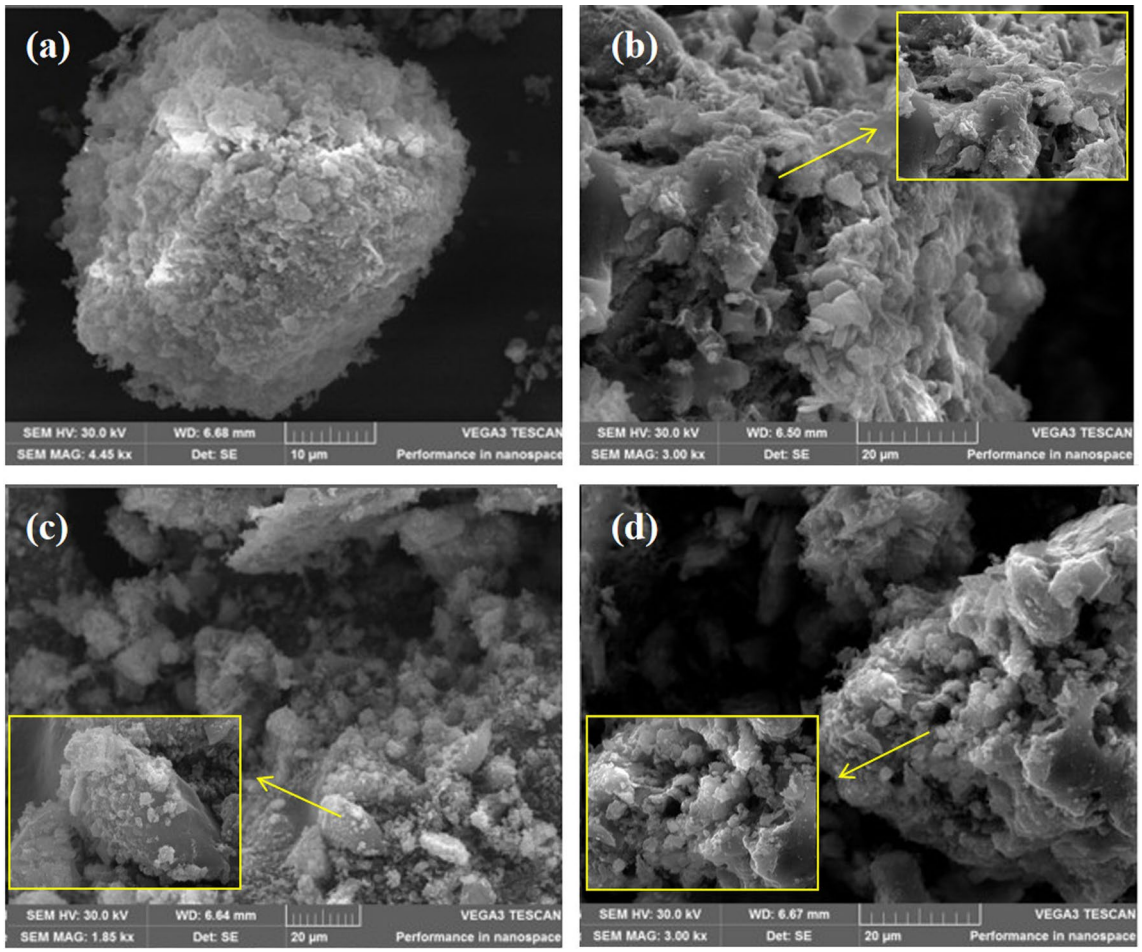

Fig. 1 Morphological structure of KOH-free biochar (**a**), 3/1 KOH-biochar (**b**), 4/1 KOH-biochar (**c**), and 5/1 KOH-biochar (**d**), by scanning electron microscopy (SEM). Magnification from 50,000 to 200,000 times, where 3/1 KOH-biochar: preparation of modified biochar with potassium hydroxide/biochar mass ratio of 3/1; 4/1 KOH-biochar: preparation of modified biochar with potassium hydroxide/biochar mass ratio of 4/1; 5/1 KOH-biochar: preparation of modified biochar with potassium hydroxide/biochar mass ratio of 5/1

pore structure of KOH-biochar changed significantly and had a complex, porous and multilayer surface structure.

Comparing the surface morphologies of biochar before and after activation, found that the surface pore structure of KOH-biochar contains a large number of pore structures and a more uneven surface structure, which is due to the reaction between activator and biochar. Literature shows that such treatment removes ash from the surface of biochar, and that potassium hydroxide can react with biochar, embedding and penetrating the surface of biochar to form new pores, effectively increasing the porosity of biochar (Koch and Dittmar 2006; Stavropoulos et al. 2008). These pores may provide an entry for the migration of phosphate onto the active sites on KOH-biochar and the large specific surface area, thus contributing to the enhanced phosphate adsorption (Xu et al. 2017). Comparison of biochar materials prepared under three different activation conditions revealed that the surface structure of KOH-biochar materials showed a small change, and therefore needs to be further investigated in conjunction with other characterization methods.

The FTIR spectra for different biochar samples are shown in Fig. 2a. The four biochar samples exhibit many absorption peaks at the range of 500 to 4000 cm^{-1}. FTIR spectra for the 3/1, 4/1 and 5/1 KOH-biochar are similar. The distinct absorption peaks around 3438 cm^{-1} are due to the hydroxyl groups –OH vibrations (Leng et al. 2015). The characteristic peak located around 1600 cm^{-1} is assigned as a –C=O stretching vibration (Zhang et al. 2019; Delgado-Moreno et al. 2021). The peak at 1420 cm^{-1} represents the O–H bond of the carboxylic acid. And the absorption peak at 1000 cm^{-1} may be ascribed to C–H tensile vibration of substituted aromatic or ash (Ding et al. 2015). The intensity of the peaks of modified biochar increases considerably, which suggests that biochar could be successfully activated by potassium hydroxide. The presence of weak peaks in the spectrum at 500–600 cm^{-1} can be attributed to the stretching

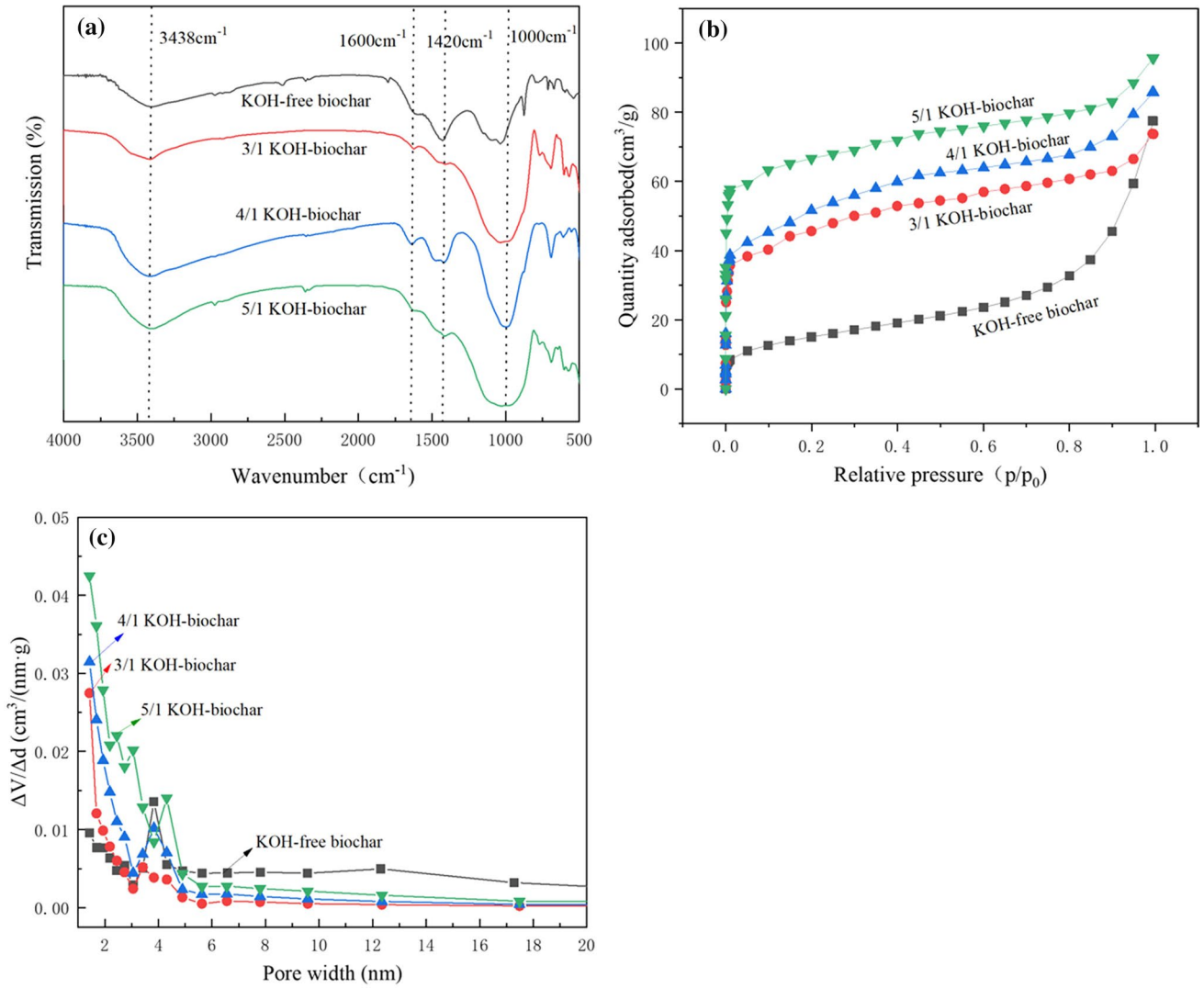

Fig. 2 **a** Fourier transform infrared spectroscopy (FTIR) of biochars at 500–4000 cm^{-1}. **b** N_2 adsorption–desorption isotherms and **c** pore size distribution curves for the KOH-free biochar, the 3/1 w/w KOH-biochar, the 4/1 KOH-biochar and the 5/1 KOH-biochar, respectively

vibrations of C–Cl of inorganic and organohalogen compounds present in the raw sludge and biochar. The peak trend is similar throughout the spectrum, indicating that the chemical bonding in the biochar is not fundamentally altered before and after modification.

The nitrogen adsorption–desorption isotherms of biochar materials are shown in Fig. 2b. Results show that the variations of the specific surface area of biochar materials follow the variation of their adsorption capacity. The adsorption capacity of several KOH-biochar materials was significantly higher than the KOH-free biochar. This is because potassium hydroxide modification can increase the specific surface area and pore size of biochar, providing space for nitrogen storage and thus improving the adsorption capacity of biochar (Bashir et al. 2018; Liu et al. 2018). However, a comparison of three KOH-biochar samples found that the adsorption trend and capacity were similar, which is due to the similarity of the principle of modifying biochar with different doses of the same activator. The pore size distribution curves of biochar materials are shown in Fig. 2c. It can be seen that biochar materials had a hierarchical pore structure. Moreover, the microporous area of KOH-biochar increased significantly, which indicated that the activation conditions had some influence on the pore size distribution of biochar. The specific parameters of the specific surface area and pore structure of biochar materials are summarized in Supplementary Table S1. It can be seen that the specific surface area of KOH-biochar materials prepared under different activation conditions ranged from 77.228 m^2/g to 85.024 m^2/g, the average pore size ranged from 1.427 nm to 2.196 nm, and the total pore volume ranged from a minimum of 0.049 cm^3/g to a maximum of 0.071 cm^3/g. However, the final

adsorption capacity of KOH-biochar materials with different amounts of activator varied. The specific surface area and pore structure parameters of 3/1 KOH-biochar, 4/1 KOH-biochar and 5/1 KOH-biochar did not differ significantly, which indicated that increasing the KOH/ biochar mass ratio of activator to biochar had some effect on the specific surface area, pore structure and adsorption performance of biochar, but the effect was independent to KOH-biochar ratios.

As shown in Table S1, the specific surface area and porosity of the biochar changed with the activation conditions. When comparing the modified biochar with the unmodified biochar, it was found that the specific surface area of the modified biochar increased, indicating that during the activation process, the activator potassium hydroxide reacted with the constituent substances in the biochar and some of the substances on the surface of the biochar were decomposed, forming a multilayer complex surface structure and increasing the specific surface area of the biochar. The increase in specific surface area contributes to the good adsorption performance of biochar samples on removal of pollutants (Rajapaksha et al. 2016).

Phosphate recovery from wastewater with alkaline potassium-modified biochar materials

The adsorption behavior of biochar materials was examined by the Langmuir and Freundlich isotherm models (Fig. 3a,b), and the calculated parameters are given in Supplementary Table S2. Results show that the Freundlich isotherms of KOH-free biochar and 3/1 KOH-biochar samples are more consistent with phosphate adsorption than the Langmuir isotherms, and the Langmuir isotherms of 4/1 KOH-biochar and 5/1 KOH-biochar are more suitable for phosphate adsorption than the Freundlich isotherms. It implied that the multilayer adsorption was the main pathway to remove phosphate toward the heterogeneous surface of the KOH-free biochar and the 3/1 KOH-biochar samples, while the phosphate adsorption process of the 4/1 KOH-biochar and the 5/1 KOH-biochar belongs to the monolayer chemisorption. The R^2 values of the two models of the four biochar samples are very similar, so it is believed that the phosphate adsorption of biochar prepared is controlled by multiple processes and has high adsorption capacity.

By analyzing the adsorption effect of modified biochar on phosphate, we observe that the adsorption capacity of four biochar materials for phosphate was in the following order: 5/1 KOH-biochar > 4/1 KOH-biochar > 3/1 KOH-biochar > KOH-free biochar; the maximum adsorption capacity of the 5/1 KOH-biochar sample was fitted by the Langmuir equation as 42.51 mg/g, compared with 27.83 mg/g for the KOH-free biochar, 37.80 mg/g for the 3/1 KOH-biochar, and 41.59 mg/g for the 4/1 KOH-biochar. The adsorption performance of modified biochar materials was significantly increased compared to the pristine biochar, indicating that hydroxide provides additional adsorption sites and greater adsorption capacity than the pristine biochar. These results are in agreement with those of Prapagdee et al. (2014).

The adsorption kinetic curves of biochar materials are shown in Fig. 3c,d, and the best-fit parameters are given in Supplementary Table S3. Results show that for four biochar materials, the calculated correlation coefficient (R^2) values by the quasi-second-order model were above 0.90 and higher than the R^2 values calculated by the quasi-first-order model. Moreover, the calculated adsorption quantities (qe) by the quasi-second-order model were better fitted with the experimental data. Therefore, the adsorption process of biochar materials was well described by a quasi-second-order model, indicating that the adsorption process was affected by chemical interactions (Wang et al. 2019). It is reported that the chemical adsorption process for biochar plays a decisive role in phosphate adsorption ability. Nutrients could be adsorbed on the surface pores and pass into the biochar; thus, the activity of biochar adsorption would gradually reduce (Xiong et al. 2017).

Performance comparison with reported modified biochar materials

To facilitate comparison with other reported phosphorus adsorbents, Table 1 summarizes the performance of other modified biochar materials used for phosphate removal from wastewater. The maximum adsorption capacity of the 5/1 KOH-biochar sample was fitted by the Langmuir equation as 42.51 mg/g versus the KOH-free biochar as 27.83 mg/g, while the maximum adsorption capacities for the 3/1 and the 4/1 KOH-biochar were 37.80 mg/g and 41.59 mg/g, respectively. Except for some costly rare earth element modified biochar materials, potassium hydroxide-modified septic tank sludge biochar materials prepared in this study are comparable to or even better than most of the previously reported phosphorus adsorbents (Feng et al. 2021; Li et al. 2020; Spataru et al. 2016). In addition, the septic tank sludge has the advantage of large annual production, wide availability and low cost, making potassium hydroxide-modified septic tank sludge-based biochar more feasible and competitive for resource recovery and economic use as a phosphorus adsorbent.

At present, there are few studies on the use of septic tank sludge for biochar preparation, and a large amount of septic tank sludge from sanitary facilities lacks systematic and standardized treatment, thus leading to environmental pollution and resource waste, which requires advanced methods to recover septic tank sludge. Our research results show that the preparation of biochar by pyrolysis of septic tank sludge and its modification by alkaline treatment of biochar with a certain percentage of potassium hydroxide can lead

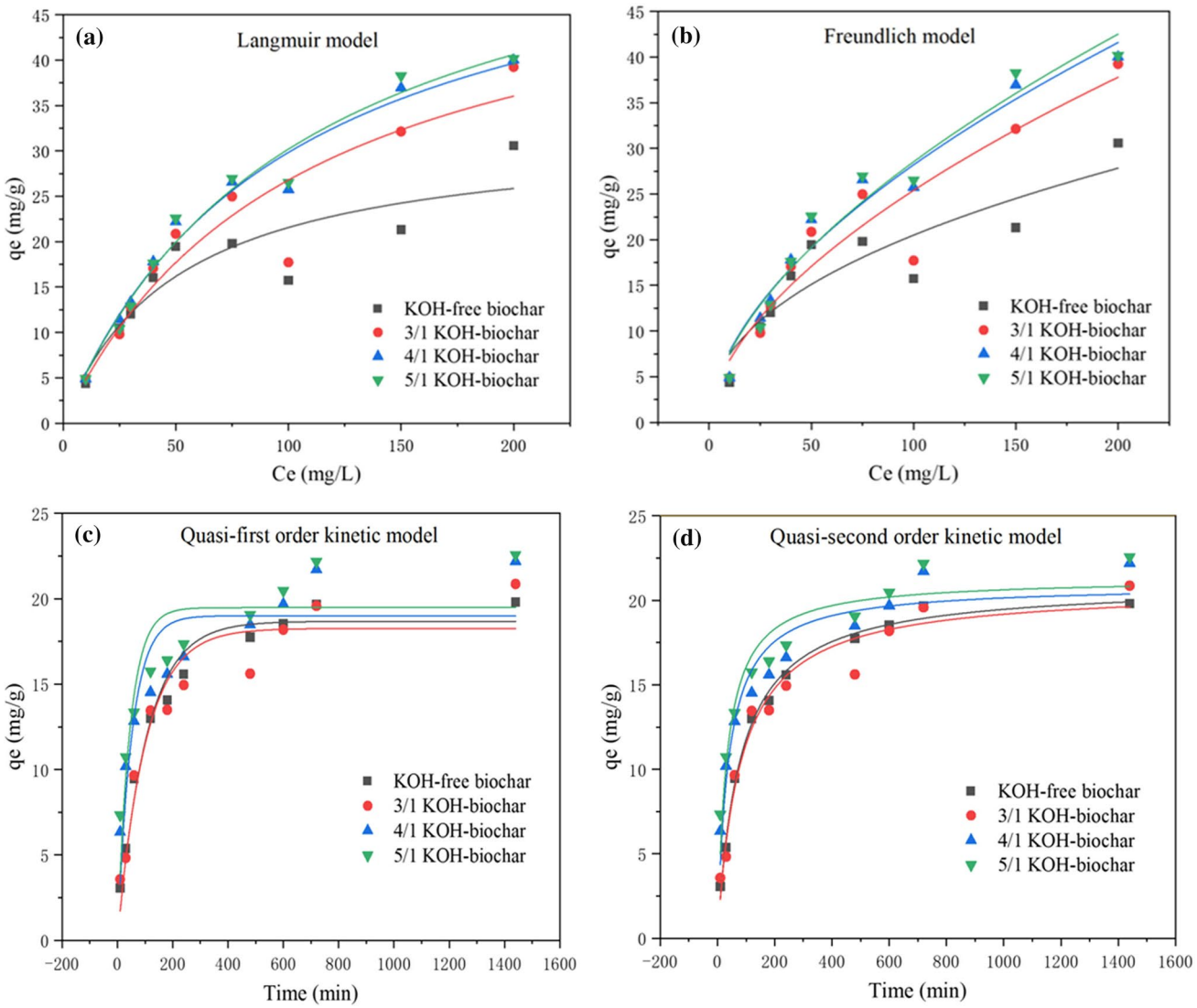

Fig. 3 Phosphate adsorption isotherms using **a** Langmuir model and **b** Freundlich model and kinetic curves using; **c** quasi-first-order kinetic models and **d** quasi-second-order models for the KOH-free biochar, the 3/1 KOH-biochar, the 4/1 KOH-biochar and the 5/1 KOH-biochar, respectively, where 3/1 KOH-biochar: preparation of modified biochar with potassium hydroxide/biochar mass ratio of 3/1; 4/1 KOH-biochar: preparation of modified biochar with potassium hydroxide/biochar mass ratio of 4/1; 5/1 KOH-biochar: preparation of modified biochar with potassium hydroxide/biochar mass ratio of 5/1

to highly efficient phosphorus adsorbent. This treatment method can not only recycle septic tank sludge, reduce the unqualified treatment of septic tank sludge, but also recover phosphorus from wastewater. By comparing the adsorption effect of the three modified biochar materials, it was found that the adsorption effect of the 5/1 KOH-biochar and the 4/1 KOH-biochar was significantly higher than that of the 3/1 KOH-biochar, while the difference in adsorption effect between the 5/1 KOH-biochar and the 4/1 KOH-biochar was insignificant. Therefore, phosphorus removal/recovery in wastewater remediation using 4/1 KOH-biochar is more environmentally and economically feasible.

Conclusion

The preparation process of the septic tank sludge-based biochar is simple and easy to operate and has low operating costs. At higher temperatures, the surface of the septic tank sludge reacted more fully to obtain a richer surface structure. After further modifications, it was found that the surface area of the modified biochar increased from 64.214 m^2/g (KOH-free) to 77.228 m^2/g, 85.024 m^2/g and 82.901 m^2/g at KOH/ biochar mass ratios of 3/1, 4/1 and 5/1, respectively. And it was also found that the medium and large pores of the biochar were transformed into microporous structures, which had a positive effect on the removal of pollutants from

Table 1 Comparison of phosphate (PO_4^{3-}) adsorption capacity among different modified biochar materials from previous reports and the present study

Raw material	Treatment temperature (℃)	Modifiers	Maximum adsorption capacity (mg/g)	References
Pine wood	500	Ferric chloride	3.20	Qiu and Duan (2019)
Sewage plant sludge	210	Potassium hydroxide	14.20	Spataru et al. (2016)
Peanut shells	600	Magnesium chloride	18.96	Wu et al. (2019)
Fragrant bushes	75	Lanthanum chloride	36. 01	Xu et al. (2019)
Septic tank sludge	500	3/1 KOH biochar	37.80	This study
Septic tank sludge	500	4/1 KOH biochar	41.59	This study
Septic tank sludge	500	5/1 KOH biochar	42.51	This study
Corn straw	300	Cerium chloride	77. 52	Feng et al. (2017)
Sheep manure	800	Lanthanum	92.67	Feng et al. (2021)
Sewage plant sludge	600	Lanthanum	93.91	Li et al. (2020)

the wastewater by the biochar. The adsorption capacity of four biochar materials for phosphate was in the following order of 5/1 KOH-biochar > 4/1 KOH-biochar > 3/1 KOH-biochar > KOH-free biochar. The maximum adsorption capacity of 5/1 KOH-biochar reached 42.51 mg/g versus 7.83 mg/g of the KOH-free biochar. In this study, the preparation of biochar by pyrolysis of septic tank sludge and alkaline treatment with potassium hydroxide can yield highly efficient phosphorus adsorbent. This treatment can not only recycle the septic tank sludge, relieve the pressure of septic tank sludge treatment, but also it can effectively recover/remove phosphorus from wastewater.

Supplementary Information The online version contains supplementary material available at https://doi.org/10.1007/s10311-022-01527-5.

Acknowledgements The authors would like to acknowledge the co-funding of this work by the National Natural Science Foundation of China (No.52070130) and the Natural Science Foundation of Shanghai (No.22ZR1443200).

Declarations

Conflict of interest The authors declare that they have no known com-peting financial interests or personal relationships that could have ap-peared to influence the work reported in this paper.

References

Ahmad M, Rajapaksha AU, Lim JE, Zhang M, Bolan N, Mohan D et al (2014) Biochar as a sorbent for contaminant management in soil and water: a review. Chemosphere 99:19–33. https://doi.org/10.1016/j.chemosphere.2013.10.071

Bashir S, Zhu J, Fu Q, Hu H (2018) Comparing the adsorption mechanism of Cd by rice straw pristine and KOH-modified biochar. Environ Sci Pollut Res 25:11875–11883. https://doi.org/10.1007/s11356-018-1292-z

Bizsel N, Uslu O (2000) Phosphate, nitrogen and iron enrichment in the polluted Izmir Bay, Aegean Sea. Mar Environ Res 49:101–122. https://doi.org/10.1016/S0141-1136(99)00051-3

Bond T, Tse Q, Chambon CL, Fennell P, Fowler GD, Krueger BC et al (2018) The feasibility of char and bio-oil production from pyrolysis of pit latrine sludge. Environ Sci Water Res Technol 4:253–264. https://doi.org/10.1039/c7ew00380c

Cha JS, Park SH, Jung S-C, Ryu C, Jeon J-K, Shin M-C et al (2016) Production and utilization of biochar: a review. J Ind Eng Chem 40:1–15. https://doi.org/10.1016/j.jiec.2016.06.002

Cheng X, Li S (2006) An analysis on the evolvement processes of lake eutrophication and their characteristics of the typical lakes in the middle and lower reaches of Yangtze River. Chin Sci Bull 51:1603–1613. https://doi.org/10.1007/s11434-006-2005-4

Delgado-Moreno L, Bazhari S, Gasco G, Méndez A, El Azzouzi M, Romero E (2021) New insights into the efficient removal of emerging contaminants by biochars and hydrochars derived from olive oil wastes. Sci Total Environ 752:141838. https://doi.org/10.1016/j.scitotenv.2020.141838

Ding S, Li Y, Zhu T, Guo Y (2015) Regeneration performance and carbon consumption of semi-coke and activated coke for SO_2 and NO removal. J Environ Sci 34:37–43. https://doi.org/10.1016/j.jes.2015.02.004

Fang C, Zhang T, Li P, Jiang R, Wu S, Nie H et al (2015a) Phosphorus recovery from biogas fermentation liquid by Ca–Mg loaded biochar. J Environ Sci 29:106–114. https://doi.org/10.1016/j.jes.2014.08.019

Fang G, Zhu C, Dionysiou DD, Gao J, Zhou D (2015b) Mechanism of hydroxyl radical generation from biochar suspensions: implications to diethyl phthalate degradation. Bioresour Technol 176:210–217. https://doi.org/10.1016/j.biortech.2014.11.032

Feng Y, Lu H, Liu Y, Xue L, Dionysiou DD, Yang L et al (2017) Nano-cerium oxide functionalized biochar for phosphate retention: preparation, optimization and rice paddy application. Chemosphere 185:816–825. https://doi.org/10.1016/j.chemosphere.2017.07.107

Feng Y, Luo Y, He Q, Zhao D, Zhang K, Shen S et al (2021) Performance and mechanism of a biochar-based Ca-La composite for the adsorption of phosphate from water. J Environ Chem Eng 9:105267. https://doi.org/10.1016/j.jece.2021.105267

Guo L, Chen A, He N, Yang D, Liu M (2018) Exogenous silicon alleviates cadmium toxicity in rice seedlings in relation to Cd distribution and ultrastructure changes. J Soils Sediments 18:1691–1700. https://doi.org/10.1007/s11368-017-1902-2

Huang R, Fang C, Lu X, Jiang R, Tang Y (2017) Transformation of phosphorus during (hydro)thermal treatments of solid biowastes: reaction mechanisms and implications for P reclamation and recycling. Environ Sci Technol 51:10284–10298. https://doi.org/10.1021/acs.est.7b02011

Isa SA, Hafeez MA, Singh BK, Kwon SY, Choung S, Um W (2022) Efficient mercury sequestration from wastewaters using palm kernel and coconut shell derived biochars. Environ Adv. https://doi.org/10.1016/j.envadv.2022.100196

Koch BP, Dittmar T (2006) From mass to structure: an aromaticity index for high-resolution mass data of natural organic matter. Rapid Commun Mass Spectrom 20(5):926–932. https://doi.org/10.1002/rcm.2386

Krueger BC, Fowler GD, Templeton MR, Moya B (2020) Resource recovery and biochar characteristics from full-scale faecal sludge treatment and co-treatment with agricultural waste. Water Res 169:115253. https://doi.org/10.1016/j.watres.2019.115253

Lei Y, Geraets E, Saakes M, van der Weijden RD, Buisman CJN (2020) Electrochemical removal of phosphate in the presence of calcium at low current density: precipitation or adsorption? Water Res 169:115207. https://doi.org/10.1016/j.watres.2019.115207

Leng L, Yuan X, Zeng G, Shao J, Chen X, Wu Z et al (2015) Surface characterization of rice husk bio-char produced by liquefaction and application for cationic dye (Malachite green) adsorption. Fuel 155:77–85. https://doi.org/10.1016/j.fuel.2015.04.019

Li Z, Jiang N, Wu F, Zhou Z (2013) Experimental investigation of phosphorus adsorption capacity of the waterworks sludges from five cities in China. Ecol Eng 53:165–172. https://doi.org/10.1016/j.ecoleng.2012.12.038

Li J, Li B, Huang H, Zhao N, Zhang M, Cao L (2020) Investigation into lanthanum-coated biochar obtained from urban dewatered sewage sludge for enhanced phosphate adsorption. Sci Total Environ 714:136839. https://doi.org/10.1016/j.scitotenv.2020.136839

Liu H, Xu F, Xie Y, Wang C, Zhang A, Li L et al (2018) Effect of modified coconut shell biochar on availability of heavy metals and biochemical characteristics of soil in multiple heavy metals contaminated soil. Sci Total Environ 645:702–709. https://doi.org/10.1016/j.scitotenv.2018.07.115

Lozano-Castelló D, Calo JM, Cazorla-Amorós D, Linares-Solano A (2007) Carbon activation with KOH as explored by temperature programmed techniques, and the effects of hydrogen. Carbon 45:2529–2536. https://doi.org/10.1016/j.carbon.2007.08.021

Nguyen DD, Ngo HH, Guo W, Nguyen TT, Chang SW, Jang A et al (2016) Can electrocoagulation process be an appropriate technology for phosphorus removal from municipal wastewater? Sci Total Environ 563–564:549–556. https://doi.org/10.1016/j.scitotenv.2016.04.045

Omwene PI, Kobya M (2018) Treatment of domestic wastewater phosphate by electrocoagulation using Fe and Al electrodes: a comparative study. Process Saf Environm Prot 116:34–51. https://doi.org/10.1016/j.psep.2018.01.005

Pandey MK, Jenssen PD (2015) Reed beds for sludge dewatering and stabilization. J Environ Prot 06:341–350. https://doi.org/10.4236/jep.2015.64034

Prapagdee S, Piyatiratitivorakul S, Petsom AJE (2014) Activation of Cassava stem biochar by physico-chemical method for stimulating cadmium removal efficiency from aqueous solution. EnvironmentAsia 7:60–69. https://doi.org/10.14456/ea.2014.25

Qiu B, Duan F (2019) Synthesis of industrial solid wastes/biochar composites and their use for adsorption of phosphate: from surface properties to sorption mechanism. Colloids Surf A Physicochem Eng Asp 571:86–93. https://doi.org/10.1016/j.colsurfa.2019.03.041

Rajapaksha AU, Chen SS, Tsang DCW, Zhang M, Vithanage M, Mandal S et al (2016) Engineered/designer biochar for contaminant removal/immobilization from soil and water: Potential and implication of biochar modification. Chemosphere 148:276–291. https://doi.org/10.1016/j.chemosphere.2016.01.043

Recalde M, Woudstra T, Aravind PV (2018) Renewed sanitation technology: a highly efficient faecal-sludge gasification–solid oxide fuel cell power plant. Appl Energy 222:515–529. https://doi.org/10.1016/j.apenergy.2018.03.175

Shepherd JG, Sohi SP, Heal KV (2016) Optimising the recovery and re-use of phosphorus from wastewater effluent for sustainable fertiliser development. Water Res 94:155–165. https://doi.org/10.1016/j.watres.2016.02.038

Sika MP, Hardie AG (2014) Effect of pine wood biochar on ammonium nitrate leaching and availability in a South African sandy soil. Eur J Soil Sci 65:113–119. https://doi.org/10.1111/ejss.12082

Spataru A, Jain R, Chung JW, Gerner G, Krebs R, Lens PNL (2016) Enhanced adsorption of orthophosphate and copper onto hydrochar derived from sewage sludge by KOH activation. RSC Adv 6:101827–101834. https://doi.org/10.1039/c6ra22327c

Stavropoulos GG, Samaras P, Sakellaropoulos GP (2008) Effect of activated carbons modification on porosity, surface structure and phenol adsorption. J Hazard Mater 151:414–421. https://doi.org/10.1016/j.jhazmat.2007.06.005

Strande L, Ronteltap M, Brdjanovic D (2014) Faecal sludge management: systems approach for implementation and operation. IWA Publishing 13:1–402. https://doi.org/10.2166/9781780404738

Strande L, Niwagaba C, Niang S, Diaw S, Diene A, Sekigongo P et al (2017) Faecal sludge as a solid industrial fuel: a pilot-scale study. J Water Sanit Hyg Dev 7:243–251. https://doi.org/10.2166/washdev.2017.089

Wang T, Zhang Z, Zhang H, Zhong X, Liu Y, Liao S et al (2019) Sorption of carbendazim on activated carbons derived from rape straw and its mechanism. RSC Adv 9:41745–41754. https://doi.org/10.1039/C9RA06495H

Wang H, Xiao K, Yang J, Yu Z, Yu W, Xu Q et al (2020a) Phosphorus recovery from the liquid phase of anaerobic digestate using biochar derived from iron−rich sludge: a potential phosphorus fertilizer. Water Res 174:115629. https://doi.org/10.1016/j.watres.2020.115629

Wang J, Lei S, Liang L (2020b) Preparation of porous activated carbon from semi-coke by high temperature activation with KOH for the high-efficiency adsorption of aqueous tetracycline. Appl Surface Sci 530:147187. https://doi.org/10.1016/j.apsusc.2020.147187

Wang Y, Miao J, Saleem M, Yang Y, Zhang Q (2022) Enhanced adsorptive removal of carbendazim from water by $FeCl_3$-modified corn straw biochar as compared with pristine, HCl and NaOH modification. J Environ Chem Eng 10:107024. https://doi.org/10.1016/j.jece.2021.107024

Wu L, Wei C, Zhang S, Wang Y, Kuzyakov Y, Ding X (2019) MgO-modified biochar increases phosphate retention and rice yields in saline-alkaline soil. J Clean Product 235:901–909. https://doi.org/10.1016/j.jclepro.2019.07.043

Wu L, Zhang S, Wang J, Ding X (2020) Phosphorus retention using iron (II/III) modified biochar in saline-alkaline soils: Adsorption, column and field tests. Environ Pollut 261:114223. https://doi.org/10.1016/j.envpol.2020.114223

Xiong X, Yu IKM, Cao L, Tsang DCW, Zhang S, Ok YS (2017) A review of biochar-based catalysts for chemical synthesis, biofuel production, and pollution control. Bioresour Technol 246:254–270. https://doi.org/10.1016/j.biortech.2017.06.163

Xu B, Chen L, Xing B, Li Z, Zhang L, Yi G et al (2017) Physicochemical properties of Hebi semi-coke from underground coal gasification and its adsorption for phenol. Process Saf Environ Prot 107:147–152. https://doi.org/10.1016/j.psep.2017.02.007

Xu Q, Chen Z, Wu Z, Xu F, Yang D, He Q et al (2019) Novel lanthanum doped biochars derived from lignocellulosic wastes for efficient phosphate removal and regeneration. Bioresour Technol 289:121600. https://doi.org/10.1016/j.biortech.2019.121600

Ye Y, Ngo HH, Guo W, Liu Y, Zhang X, Guo J et al (2016) Insight into biological phosphate recovery from sewage. Bioresour Technol 218:874–881. https://doi.org/10.1016/j.biortech.2016.07.003

Zhang J, Shao J, Jin Q, Li Z, Zhang X, Chen Y et al (2019) Sludge-based biochar activation to enhance Pb(II) adsorption. Fuel 252:101–108. https://doi.org/10.1016/j.fuel.2019.04.096

Supplementary Material for

Efficient phosphate recycling by adsorption on alkaline sludge biochar

Zehui Liu[1a], Hongbo Liu[1*a], Yi Zhang[a], Eric Lichtfouse[b]

a School of Environment and Architecture, University of Shanghai for Science and Technology, 516 Jungong Road, 200093, Shanghai, China. b Aix-Marseille Univ, CNRS, IRD, INRA, CEREGE, 13100 Aix en Provence, France

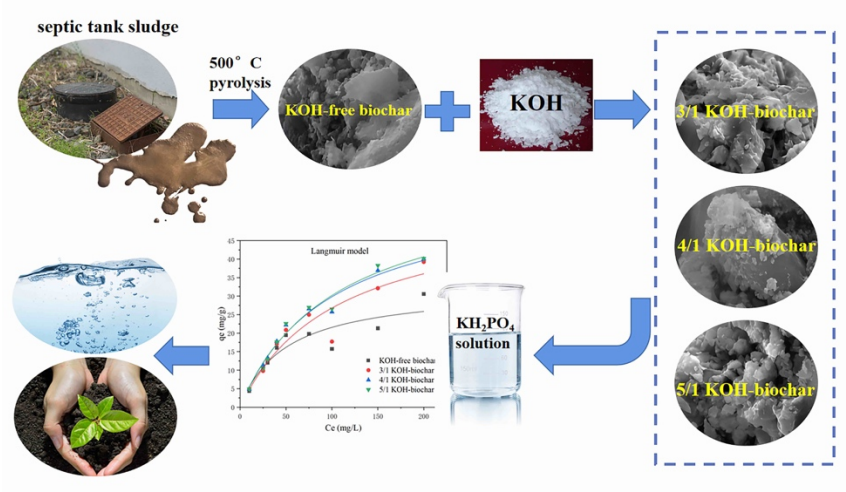

Scheme S1 Preparation of alkaline biochars from septic tank sludges for adsorption of phosphates in water. Phosphate-loaded biochar can then be used a soil amendment to fertilize plants and sequester carbon.

Table S1 Specific surface area and pore structure parameters of biochars

Samples	Specific surface area (m^2/g).	Total pore volume (cm^3/g)	Aperture (nm)	Average pore size (nm)
KOH-free biochar	64.214	0.122	3.833	9.01
3/1 KOH biochar	77.228	0.049	1.736	4.54
4/1 KOH biochar	85.024	0.071	1.427	3.27
5/1 KOH biochar	82.901	0.063	2.196	7.17

Table S2 Fitting parameters of the phosphorus adsorption isotherms of different biochars

	Langmuir			Freundlich		
	Q	K	R^2	k	n	R^2
KOH-free biochar	32.31	0.02	0.79	2.69	2.27	0.80
3/1 KOH-biochar	55.04	0.01	0.86	1.81	1.74	0.88
4/1 KOH-biochar	59.12	0.01	0.97	2.13	1.78	0.96
5/1 KOH-biochar	62.03	0.01	0.97	2.01	1.74	0.95

Table S3 Parameters of P adsorption kinetics.

	Quasi-first-order			Quasi-second-order		
	K_1	Q_1	R^2	K_2	Q_2	R^2
KOH-free biochar	0.01	18.67	0.96	6.09	20.99	0.99
3/1 KOH-biochar	0.01	18.25	0.90	6.02	20.71	0.96
4/1 KOH-biochar	0.02	19.00	0.75	0.001	20.90	0.91
5/1 KOH-biochar	0.02	19.47	0.75	0.001	21.29	0.90

* Corresponding author ADD: 516, Jungong Road, 200093, Shanghai, China. Email: Liuhb@usst.edu.cn (H., Liu)